Nanoscale Reports

RESEARCH ARTICLE

Eleyon Publishers

DOI:10.26524.nr.4.5

4(1) (2021) 25-34

OPEN ACCESS

Synthesis and Characterization of Cu Doped Mn nanoparticles by Co – Precipitation Method

V. Sabari [1], P.Praveena[1], B.Prabavathi [1], E. Ashwini [1], E. Komathi [1]

Abstract

The Cu doped Mn nanoparticles were synthesized by Co - Precipitation method. The synthesized samples are characterized by X-ray diffraction, Scanning Electron Microscope, Fourier transform infrared spectrometer, Energy-dispersive X-Ray spectroscopy and UV-V is spectrometer. The XRD studies of the sample confirmed the formation of hexagonal structure. No impurity phase was observed in the XRD. The crystallite size and lattice constants were analysed. The XRD patterns show that the average particle size is in the range of 14 nm for annealed temperature at 400°C. SEM results show both the presence of agglomeration and non agglomeration of the smaller crystallites. The EDS result exhibits the presence of Cu, Mn and O by the appearance of Mn and O peaks. This is the simple synthesis method and they are used to optical and gas sensor applications. solar cells, photocatalysis, chemical sensors, optical filters, surperionic materials, nanometer-scale switches, high-capacity cathode material in lithium secondary batteries, superconductor.

Keywords: X-ray diffraction, Scanning Electron Microscope, Energy-dispersive X-Ray spectroscopy, Co-Precipitation method.

Author Affiliation: [1]Department of Physics, Marudhar Kesari Jain College for Women,Vaniyambadi, Tamilnadu, India – 635 751.

Corresponding Author: V. Sabari.Department of Physics, Marudhar Kesari Jain College for Women,Vaniyambadi, Tamilnadu, India – 635 751.

Email: vrsabari86@gmail.com

How to cite this article: V. Sabari, Synthesis and Characterization studies of pure Mg and Cu Doped MgO Nanoparticles by Co-Precipitation Method 4(1), 25-34 Retrieved from https://nanoscalereports.com/index.php/nr/article/view/68

Received: 5 March 2021 **Revised:** 8 April 2021 **Accepted:** 10 April 2021

I.INTRODUCTION

Pure CuO is one of the most typical p-type metal-oxide semiconductors [1,2] and exhibits interesting antiferromagnetic ordering below its Néel temperature of 225 K. It has been proved that the Mn ion is an excellent magnetic dopant.[3,4] Recently, doping the Mn ions into the monoclinic lattice to substitute for a fraction of the Cu ions has been shown to make CuO possess DMS properties.[5] Since our discovery of the ferromagnetic characteristic of bulk Mn-doped CuO synthesized through a co-precipitation method followed by the annealing process.[6]

A few reports have been published on the fabrication of Mn-doped CuO with different morphologies in different ways. Hussain et al have synthesized Mn-doped CuO nanoparticles by the co-precipitation method and analyzed their ferromagnetism origin.[4] Sharma et al have prepared Mn-doped CuO amorphous nanoparticles by a hydrothermal method and then studied their weak ferroelectricity and ferromagnetism properties.[7] Zhu et al have fabricated highly (111) oriented Mn-doped CuO thin films on a thermally oxidized silicon substrate by radio-frequency magnetron sputtering. [7] Gülen et al have deposited Mn-doped CuO thin films on glass substrates via a successive ionic layer adsorption and reaction method and measured their optical band gaps. [8] Recently, Mn-doped CuO with the nanowire morphology has been successfully synthesized in our group through thermal oxidization of Mn–Cu alloys.[9] CuS is an important p-type semiconductor among the metal chalcogenides with its interesting morphology and has been extensively used in many applications like solar cells, catalysis, photocatalysis, chemical sensors, optical filters, surperionic materials, nanometer-scale switches, high-capacity cathode material in lithium secondary batteries, superconductor, thermoelectric cooling material and ideal for solar energy absorption. [10-15]

CuS nanocrystals, such as nanoparticles, nanorods and tubular crystals have been synthesised by solid-state reactions, irradiation, sonochemical, hydrothermal, solvothermal and chemical vapour deposition methods. [16-23] Compared with the synthetic methods above, solvothermal method has been increasingly used as a low-cost, low-risk and easy-to operate synthetic technique. The green CuS is attractive since it has additional absorption band in near-infrared region(NIR). [13,24,25] Moreover, CuS exhibits low reflectance in the visible and relatively high reflectance in the NIR, which makes it a prime candidate for solar energy adsorption.[26] CuS has a direct band gap of 1.2-2.0 eV [27] hence, has been extensively applied in industry, for instance, photocatalytic degradation of organic pollutants and biology markers.

In recent years, semiconductor photocatalysis technology, which provides a relatively simple method for the chemical conversion of solar energy, has received considerable attention because of its application for water splitting and the elimination of chemical contaminants.[22,28,29]

Dyes are major class of organic compounds, which find a multitude of applications in human life.[30] Most of the synthetic dyes are toxic, non-biodegradable and resistant to direct degradation by sunlight and consequently, they appear as a class of persistent pollutants. [31]

2. Experimental details

2.1. Materials

Copper (II) sulphate pentahydrate, Manganese (ll) chloride and reagents included NaOH are used for the synthesis of MnO_2 nanoparticles. All chemicals, double distilled water and reagents used were procured from Sigma-Aldrich (United States of America) and Merck (Germany) and were of analytical grade.

2.1.1 Manganese (II) chloride properties

Manganese (II) chloride is dichloride salt of manganese, $MnCl_2$. This inorganic chemical exists in anhydrous form, as well as the dehydrate ($MnCl_2.2H_2O$) and tetrahydrate ($MnCl_2.4H_2O$), with the tetrahydrate is the common form. Like many Mn (II) species, these salts are pink, with the paleness of the color being characteristic of transition metal complexes with high spin d^5 configurations.

2.1.2 COPPER (II) SUPHATE PENTAHYDRATE

The copper (II) sulfate pent hydrate is given by chemical formula $CuSO_4.5H_2O$. This form is characterized by its bright blue colour. However, it can be noted that the anhydrous form of this salt is a powder. The copper (II) sulfate pent hydrate ($CuSO_4.5H_2O$) crystals have a triclinic structure. The pent hydrate of this compound, $CuSO_4.5H_2O$ is used as a fungicide due to its ability to kill several fungi. It is also used to test the blood samples for diseases like anemia .It is also be used as a decorative since it can add colour to cement , ceramics, and other metal as well.

2.1.3 SODIUMHYDRA OXIDE PROPERTIES

Sodium hydroxide is an alkali which is also known as caustic soda. Caustic means “burning” and Caustic soda takes its name from the way it can burn the skin. It has the chemical formula of NaOH. It dissolves easily in water, and makes the water warm when this happens. Sodium hydroxide is used as a solution to make soap. It has the dissolving properties and its ability to easily break surface tension is fundamental fruits uses. It works in two ways. First, it combines with grease to make soap. Secondly, it dissolves hair (which is soluble in any basic solution).

2. 2. Sample Preparation

Copper doped manganese nanoparticles were synthesized by using Co-precipitation method. To prepare copper doped manganese nanoparicle 2.49gm of copper II sulphate pent hydrate and 25.168gm of Manganese chloride are dissolved in 100ml of distilled water and this solution was stirred using a magnetic stirrer and afterwards was added 50ml of NaOH (precipitating agent) solution was added drop by drop wise into the above solution. The above colloidal solution was stirred at

Table 1 Manganese chloride properties.

Chemical Formula	$MnCl_2$
Molar mass	125.844g/mol
Appearance	Pink crystals or crystalline powder
Crystal structure	Tetra hydrate
Density	2.98g/cm³
Melting Point	654°C(1,209°F)
Boiling point	1,225°C (2,237°F)
Solubility in water	63.4g/100ml
Solubility	Slightly soluble in pyridine, soluble in ethanol.

Table 2 Copper (II) sulphate pentahydrate properties

Chemical formula	$CuSO_4.5H_2O$
Molar mass	249.685g/mol
Appearance	Bright blue colour
Crystal structure	Triclinic
Density	2.286g/cm³
Melting point	110°C
Boiling point	150°C
Solubility in water	148g (0°C)
Solubility	Methanol

room temperature for 2 hours under constant stirring. Finally pink colour precipitate was formed. The formed nanoparticles are washed several times with distilled water and then followed by ethanol. The purpose of washing precipitate with ethanol was to remove the unwanted salt and impurities. Then the sample was dried at oven 123^{o}C for 12 hours. Finally copper doped manganese nanoparticles were obtained.

To investigate the effect of different concentrations of Cu dopant ions on the physical, chemical, and optical properties of Cu-doped MnO nanoparticles, the same procedures as stated above were carried out for 0.2mol%, 1mol%, of Cu doped MnO nanoparticles. The flow chart of the Cu doped Manganese (ll) chloride nanoparticles synthesized by simple Co-precipitation method is shown in Fig.1.

2.3. Sample Characterization.

X-Ray diffraction patterns (XRD) are generally used to determine the mean size of nanoparticles by using Scherer's equation. The microstructure of the synthesized sample was analyzed by XRD pattern recorded using a Bruker AXS D8 Advance instrument with the monochromatic CuKα1 wavelength of 1.5406 Å with a 2θ scanning range of 20°- 50°. The FTIR spectrum confirms the formation of manganese oxide. For Cu doped there is slight shift in spectrum. The FT-IR spectra of the samples were recorded in order to identify the functional groups present in the sample by using Perkin Elmer Spectrum-1, instrument resolution up to 1.0 cm^{-1}. The grain sizes estimated from (SEM) observations were different from those done by means of Scherer's equation. This equation assumes that all the crystallites are of the same size, but in actual specimen, the size range and distribution affect β . The morphological studies and energy dispersive X-ray analysis of MnO_2 have been performed with a JEOL 5600LV microscope at an accelerating voltage of 10 kV. The optical transmittances of manganese oxide nano particle were studies by UV-Vis spectroscopy. The DRS spectra of the MnO_2 samples are recorded on a Perkin Elmer UV-Visible DRS Spectrophotometer in view of identifying the metallic state of Mn. Energy-dispersive X-Ray spectroscopy (EDS) is an analytical technique used for the elemental analysis or chemical characterization of a sample. The fundamental principle that each element has a unique atomic structure allowing a unique set of peaks on its electromagnetic emission spectrum.

3. Results and Discussion

3.1. X-ray diffraction

The XRD data was investigate to know the structural change after addition of Cu doped MnO_2 nanoparticles by using Co-precipitation method. Fig.2 shows X-ray diffraction spectrum of 0.2M and1.0M of Cu doped MnO_2. This analysis identifies the existence of main diffraction planes for 0.2M of MnO_2 namely (100), (002), (101), (102), (110), (103) and (112) as the hexagonal structure (JCPDS, No.36-1451). Dasari Ayodhya et al the report that The products obtained from experiments with varying concentration of XG and uncapped CuS NPs show similar XRD patterns with a hexagonal structure. [32]

The XRD patterns of the Cu doped MnO_2 powder shows

Table 3 Sodium hydra oxide properties

Chemical formula	NaOH
Molar mass	39.9971gmol^{-1}
Crystal structure	Opaque crystal
Density	2.13g/cm^3
Melting point	318^{o}C
Boiling point	1,388^{o}C
Solubility in water	418g/L(0^{o}C)
Appearance	White, Waxy
Solubility	Glycerol, Propylene, glycol.

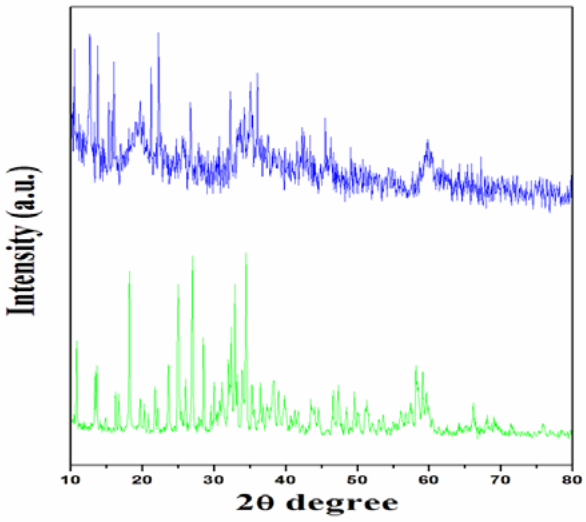

Fig.2 X-Ray diffraction patterns of Cu doped MnO2 nanoparticles with 0.2 mol% and 1mol%

that the presence of a new single peak at 1.0M doping level is emerged for a (200) plane are observed. At the same time, no other characteristic peaks from impurities are detected in the diffraction patterns of Cu doped MnO_2 samples. The XRD patterns show that Cu doping changes the growth orientation of the crystallites which is related to the particles nucleation process. It is identified from the peak (101) intensity from the Fig2 which increases sharply with adding 1.0M of Cu doping and decrease gradually with further increasing in the doping concentration. It assumed that there is a presence of only one phase because the quantity of dopent is too small as compared to the precursors of Cu and electro negativity difference between Cu and O is greater than that between Cu doped MnO_2.

The lattice spacing (d), angle of diffraction (2θ), full width at half maximum (β) and the identified nanocrystalline 0.2M and1.0M of Cu doped MnO_2 samples (hkl) plane waves. It shows that the value of full width at half maximum (FWHM) of the 0.2M and 1.0M Cu doped MnO_2 nano crystalline sample in this table is higher than 1.0M Cu doped MnO_2 and pure Mn crystalline planes. Thus this increase in FWHM confirms the reduction in crystalline size.

The lattice parameter of a and c calculated using Eq. (1) for the nano crystalline peaks.

$$\frac{1}{d^2} = \frac{4}{3}\left(\frac{h^2 + hk + k^2}{a^2}\right) + \frac{l^2}{c^2} \qquad (1)$$

It is observed that the lattice constant value of Cu doped MnO_2 nano crystalline is almost same as the JCPDS data.

The crystalline size (D) of these samples are estimated using following Scherrer's formula (2),

$$D = \frac{0.9\lambda}{\beta \cos\theta} \qquad (2)$$

Where D is the crystalline size, λ is the wavelength of X-rays used; β is the broadening of diffraction line measured at half its maximum intensity and θ is the angle of diffraction. The calculated average crystallite sizes of 0.2M of Cu doped MnO_2 in 34 nm. Similarly, the average crystalline size of 1.0M Cu doped MnO_2 is 29 nm for 0.2M dopent levels are respectively. This calculated average crystalline size reveals that there is a decrease in crystalline size at the higher doping Cu doped MnO_2 concentration in Mn.

3.2. Scanning electron microscopy (SEM)

The surface morphology of pure Mn and Cu doped MnO_2 nanoparticles were illustrated using scanning electron microscope (SEM) images as shown in Fig.4.2(a) The change in morphologies were observed for Cu doped MnO_2 nanoparticles at 0.2M and 1.0M doping concentration and it is shown in Fig. 3(a) and (b) The significant nanostructure change in the sample is observed by adding Cu doped MnO_2 nanoparticles. Agglomerated a very few rods Along with some crystalline structure are also observed in all these Cu doped MnO_2 nanoparticles samples.

3.3. Energy Dispersive Spectrum (EDS)

The Energy dispersive spectrum analysis Fig.4 is performed to investigate the elemental composition of pure Mn and Cu doped MnO_2 nanoparticles. [33] The analysis confirmed the presence of Mn, Cu and O elements in the nanostructures. Fig.4. Exhibits pure Mn spectrum with high intense peaks and single small peak which are associated with O a Mn atom, respectively.

3.4 FOURIER TRANSFORM INFRARED SPECTROSCOPE

FTIR is one of the most prominent and broadly used spectroscopic methods for analyzing the structure of unknown component. It is used to find out the functional group internal structure of molecule. The FTIR spectra of Cu doped Manganese oxide Nanoparticle is shown in Fig 5(a & b).FTIR analysis is a suitable technique to evaluate the functional groups present in the samples subjected to analysis. Fig 5 (a&b) shows the FTIR spectra of MnO_2 of different mol concentration 0.2M and 1.0M samples. The sample shows absorption bands for 0.2M at about 1116.45 $cm^{-1}$and 1194.37cm^{-1} can be attributed to C-O bond stretching and C-H bending vibration respectively indicating the presence of carbon, oxygen and hydrogen are present in the structure.

The absorption band for 1.0M at about 895.53cm^{-1} and 1409.99cm^{-1}can be attributed to C=O bond stretching and C-H bending (alkenes) vibrations . whereas the absorption band approximately 1642.63cm^{-1} was attributed to normal C=N stretching vibration takes place.Oxides and hydroxides of metal nanoparticles are generally gives absorption peak in the finger print region i.e., below wavelength of 1000nm arising from the inter-atomic vibrations. The bands at 1116.45 and 895.53cm^{-1} corresponds to Mn-O bond .from the above result we can conclude that the synthesized nanoparticle is Manganese oxide. The appearance of the diffraction patterns to correlate the bond portions number of absorption peaks to the crystalline structure.

3.5 UV-Visible Spectroscopy

The optical band gap is determined from UV-visible DRS of the MnO2 nanoparticles by using the optical absorption technique on reflectance band. The reflectance values are transformed to combination by use the Kubelka-Munk function.[34-37] The Kubelka-Munk theory is normally used for analyze the diffuse reflectance spectra obtained from inadequately interesting samples. The formula can be expressed by the subsequent relation. [38]

$$K = \frac{(1-R)^2}{2R} \qquad (3)$$

Where K is the reflectance transformed according to the Kubelka Munk and R is the reflectancy (%). The relationship between $(k * h\vartheta)^{1/2} = f(h * \vartheta)$ of MnO_2 nanoparticles. The optical characterization of the sample was recorded on UV-Vis absorption spectrum. Fig 6 (a & b) shows UV Vis spectrum of manganese oxide nanoparticles as a function of wavelength. [39]

Fig 6 (a & b) shows UV-Visible spectra of manganese oxide metal nanoparticles synthesized by co-precipitation method as a function has wavelength. [40,41] The UV-Visible absorption shows sharp absorption at 336.31nm and 339.11nm due to manganese oxide metal nanoparticles. [42,43]

CONCLUSION

The Mn and Cu doped MnO_2 nanoparticles were prepared by Co – precipitation method. The change in structural properties due to the presence of Cu doped MnO_2 was identified from the

peak (101). SEM analysis confirmed that the doping with Cu modified the morphology of nanoparticles. The calculated average crystallite sizes of 0.2M of Cu doped MnO_2 in 34 nm. Similarly, the average crystalline size of 1.0M Cu doped MnO_2 is 29 nm for 0.2M dopent levels are respectively. This calculated average crystalline size reveals that there is a decrease in crystalline size at the higher doping Cu doped MnO_2 concentration in Mn. The FTIR spectrum confirms the formation of manganese (II) chloride .Metal oxygen bond metal vibration are found around. For Cu doped there is a slight shift in spectrum around 1090.75 cm^{-1}. The optical transmittance of Manganese oxide nanoparticles were studied by UV-Visible spectroscopy. Furthermore, Cu doped MnO_2 nanoparticles have the crystallite size in

Similarly, the average crystalline size of 1.0M Cu doped MnO_2 is 29 nm for 0.2M dopent levels are respectively. This calculated average crystalline size reveals that there is a decrease in crystalline size at the higher doping Cu doped MnO_2 concentration in Mn. The FTIR spectrum confirms the formation of manganese (II) chloride .Metal oxygen bond metal vibration are found around. For Cu doped there is a slight shift in spectrum around 1090.75 cm^{-1}. The optical transmittance of Manganese oxide nanoparticles were studied by UV-Visible spectroscopy. Furthermore, Cu doped MnO_2 nanoparticles have the crystallite size in the range ~24-38 nm, as confirmed by SEM. This synthesis method is simple and cost effective approach to produce Cu doped MnO_2 nanoparticles it has used for gas sensor applications.

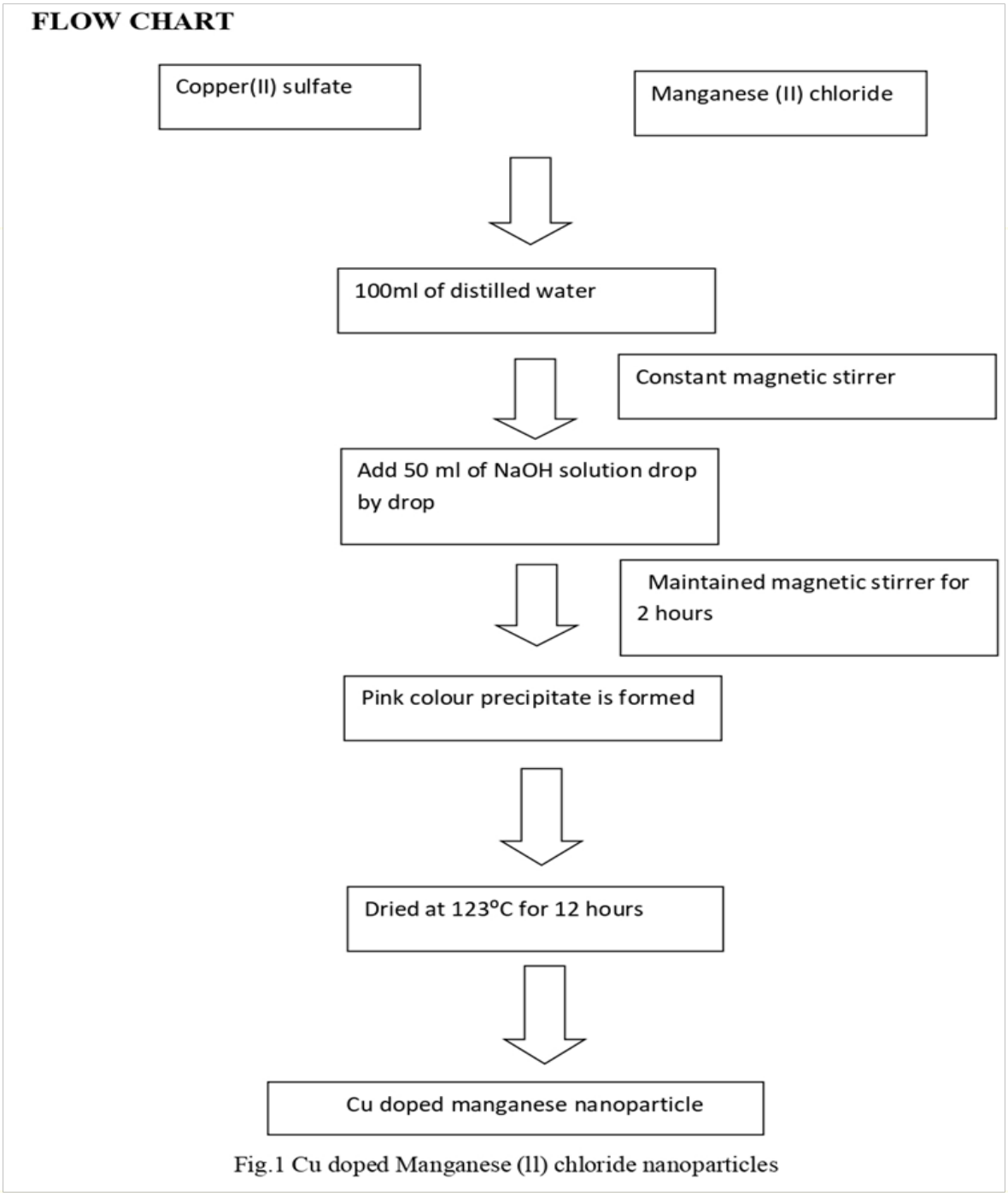

Fig.1 Cu doped Manganese (ll) chloride nanoparticles

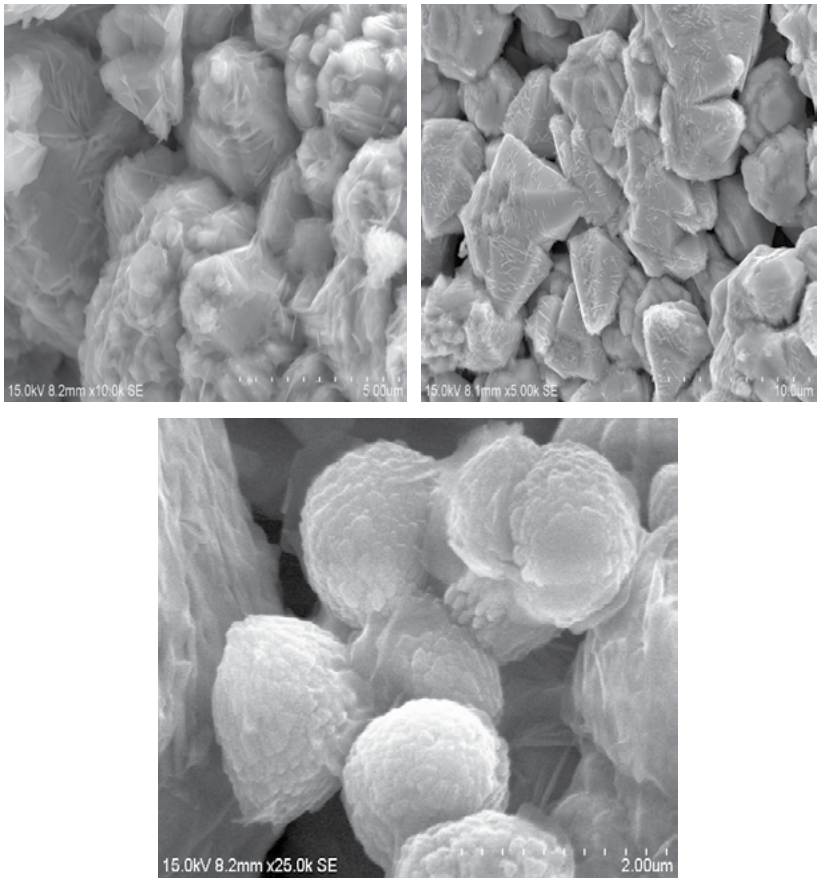

Fig.3 a) SEM images of Cu doped MnO2 nanoparticles at 0.2M

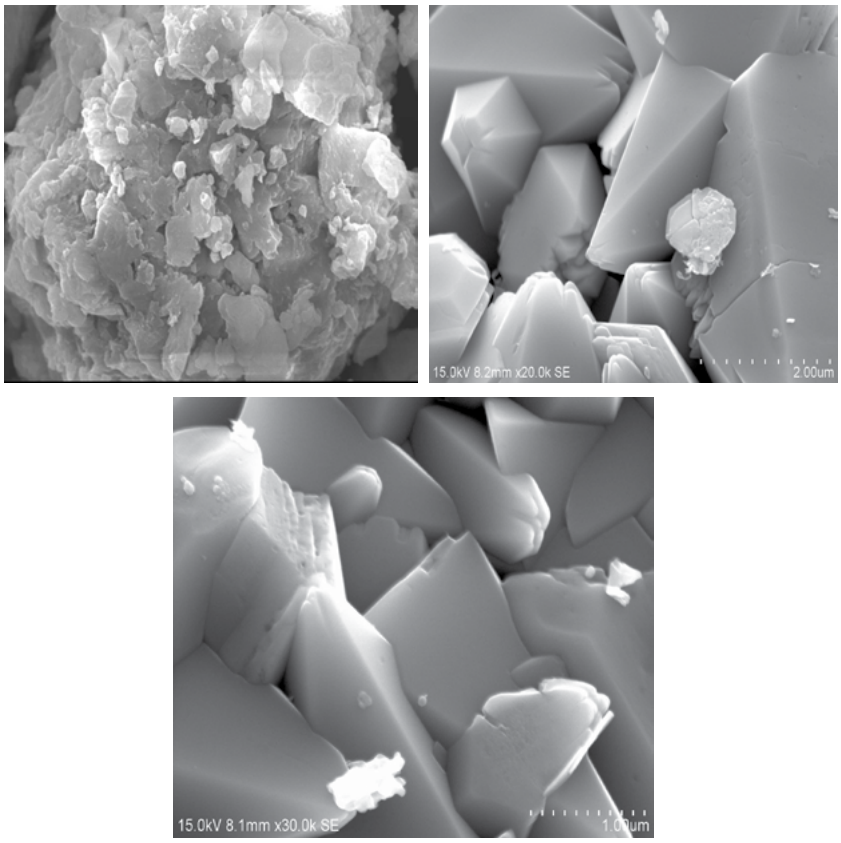

Fig3(b) SEM images of Cu doped MnO2 nanoparticles at 1.0M

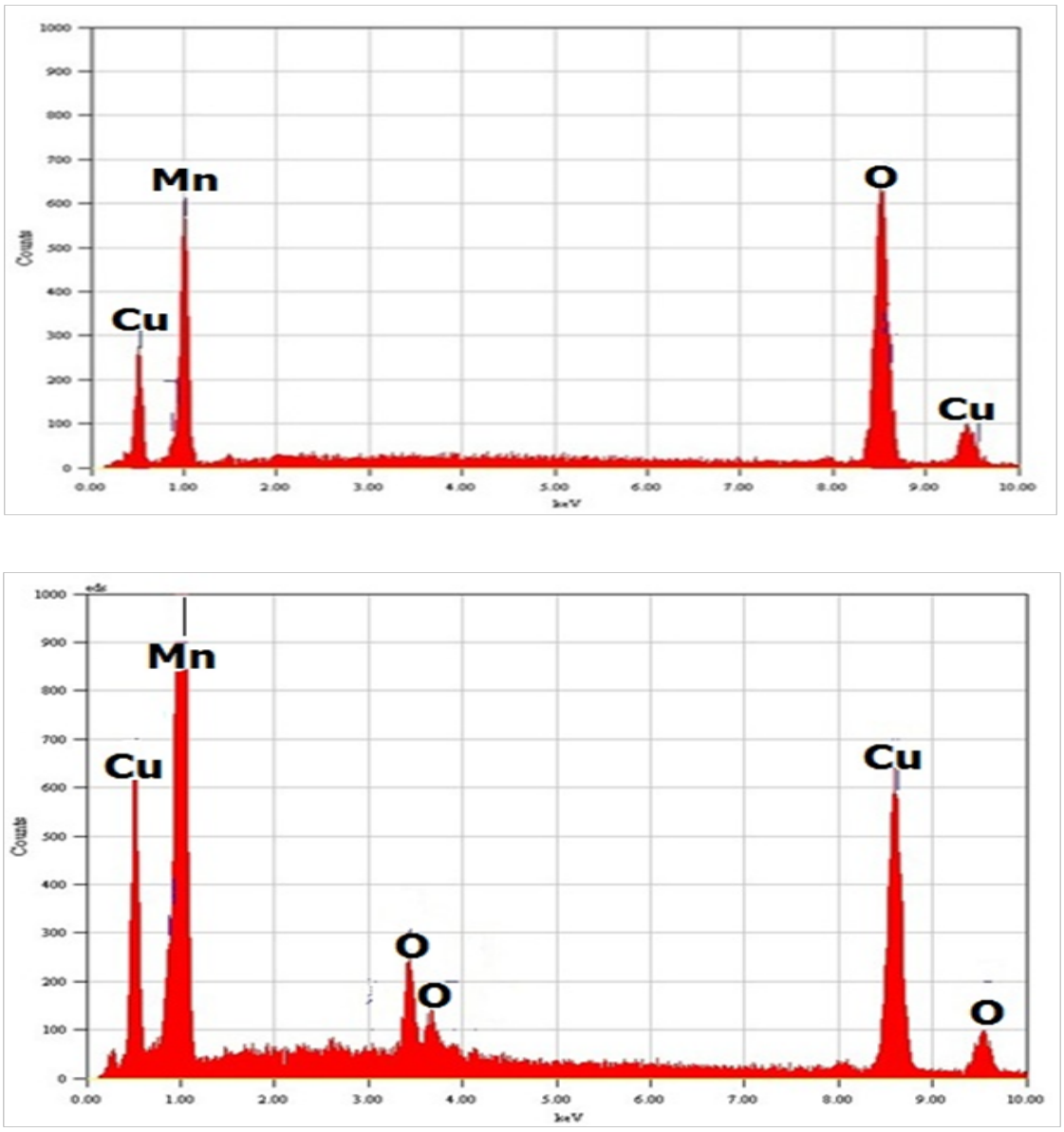

Fig.4 EDS spectrum of Cu doped MnO2 nanoparticles at 0.2M and 1.0M

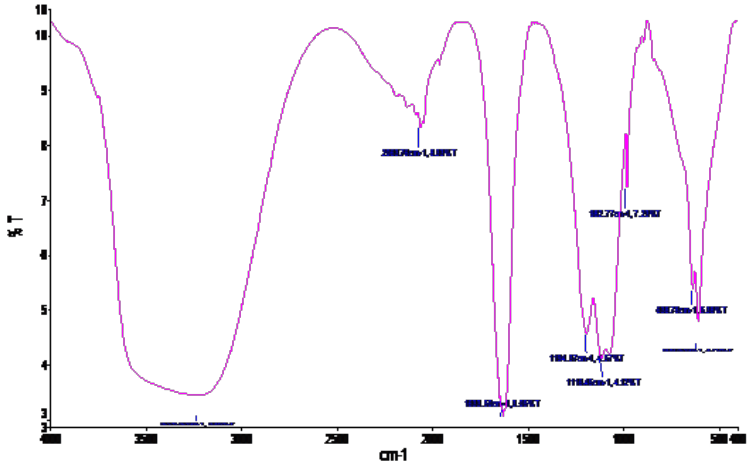

Fig 5 (a) FTIR spectrum of manganese oxide at 0.2M

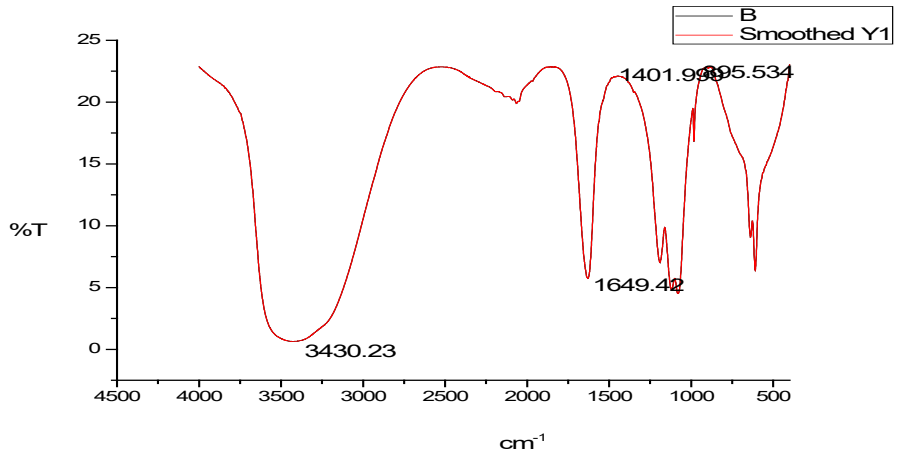

Fig 5 (b) FTIR spectrum of manganese oxide 1.0 M

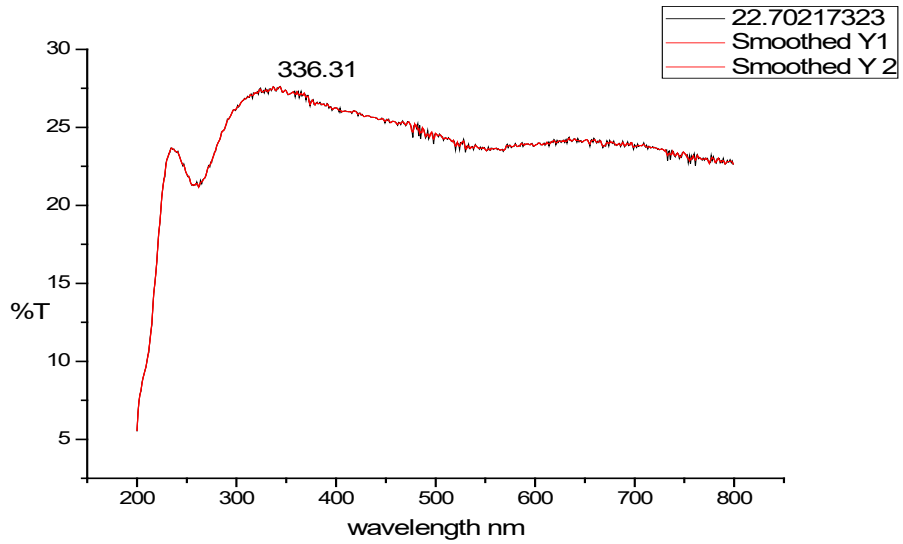

Fig 6(a) Transmittance graphs of manganese oxide at 0.2M

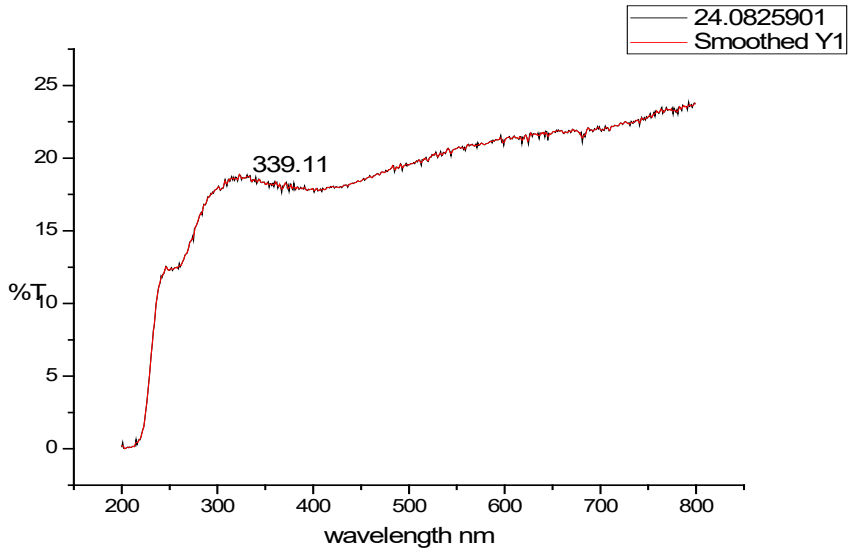

Fig 6(b) Transmittance graph of Manganese oxide at1.0M

Data Availability

The data used to support the findings of this study are included within the article. More information could be obtained from the authors upon request.

Conflicts of Interest

The authors declare that there is no conflict of interest regarding the publication of this paper.

Acknowledgments

The authors would like to thank management, principal and head of the department for their continues support and encouragement for making this article successful as part of my research.

Funding

No funding was received to carry out this study.

References

1. S. Iqbal, R.K. Bedi Appl. Surf. Sci, 257(17) (2011) 7592-7599.
2. R. Sahay, J. Sundaramurthy,P.S. Kumar, V. Thavasi, S.G. Mhaisalkar, S. Ramakrishna, J. Solid State Chem, 186 (2012) 261-267.
3. J.T. Arantes, A.J.R. Da Silva, A. Fazzio, Phys. Rev, (2007).
4. S. Patibandla, Spin transport studies in nanoscale spin valves and magnetic tunnel junctions PhD Thesis Virginia Commonwealth University See : (http://scholarscompass.vcu.edu/cgi/viewcontent.cgi ?article= 2610&context=etd), (2008).
5. F. Zhao, H.M. Qiu, L.Q Pan, H. Zhu, Y.P. Zhang, Z.G. Guo, J.H. Yin, X.D. Zhao, J. Xiao,Q J. Phys.: Condens. Matter, (2008).
6. S. Hussain, A. Mumtaz, S.K. Hasanain, M. Usman, J. Appl. Phys, (2012).
7. N. Sharma, A. Gaur, R.K. Kotnala, J. Magn. Magn. Mater, (2015).
8. H. Zhu, F. Zhao, L.Q. Pan, Y.P. Zhang, C.F. Fan , Y. Zhang, J.Q. Xiao, J. Appl. Phys, (2007).
9. Y. Gülen, F. Bayansal, B. Sahin, H.A Cetinkara, H.S. Guder, Ceram Int, (2013).
10. W.L. Gao, S.H. Yang, S.G. Yang, L.Y. Lv, Y.W. Du, Phys. Lett, (2010).
11. Y. Wu, C. Wadia, W. Ma, Synthesis and photovoltaic application of copper (I) sulfide nanocrystals. Nano Lett, 8 (2008) 2551-2555.
12. H. Xu, W. Wang, W. Zhu, Sonochemical synthesis of crystalline CuS nanoplates via an in situ template route. Mater Lett, 60 (2006) 2203-2206.
13. L.Z. Pei, J.F. Wang, X.X. Tao, Synthesis of CuS and Cu1.1Fe1.1S2 crystals and their electrochemical properties. Mater Characterization, 62 (2011) 354-359.
14. K.J. Wang, G.D. Li, J.X. Li, Formation of single-crystalline CuS nanoplates vertically standing on flat substrate. Crystal Growth Des, 7 (2007) 2265-2267.
15. S. Xu, Q. Wang, J.H. Cheng, Preparation and characteristics of porous CuS microspheres consisted of polycrystalline nanoslices, Powder Technol, 199 (2010) 139-143.
16. J. Lu, Y. Zhao, N. Chen, et al. A novel in situ template-controlled route to CuS nanorods via transition metal liquid crystals, Chem Lett,32 (2003) 30-31.
17. C. Wang, K. Tang, Q. Yang, Synthesis of CuS millimeter-scale tubular crystals. Chem Lett, 30 (2001) 494-495.
18. P. Zhang, L.Gao, Copper sulfide flakes and nanodisks. J Mater Chem, 13 (2003) 2007-2010.
19. C.Y. Wu, S.H. Yu, S.F. Chen, Large scale synthesis of uniform CuS nanotubes in ethylene glycol by a sacrificial templating method under mild conditions. J Mater Chem, 16 (2006) 3326-3331.
20. A.M. Qin, Y.P. Fang, H.D. Ou, Formation of various morphologies of covellite Copper sulfide submicron crystals by a hydrothermal method without surfactant. Crystal Growth Des, 5 (2005) 855-860
21. H.T. Zhang, G. Wu, X.H. Chen, Controlled synthesis and characterization of covellite CuS) nanoflakes, Mater Chem Phys, 98 (2006) 298-303.
22. H.M. Ji, J.M. Cao, J. Feng, Fabrication of CuS nanocrystals with various morphologies in the presence of a nonionic surfactant. Mater Lett, 59 (2005) 3169-3172.
23. C.H. Tan, Y.L. Zhu, R. Lu, Synthesis of copper sulfide nanotube in the hydrogel system.Mater Chem Phys, 91 (2005) 44-47.
24. Y. Zhao, H. Pan, Y. Lou, Plasmonic Cu2-xS nanocrystals: optical and structural properties of copper-deficient copper(I) sulfides. J Am Chem Soc, 131 (2009) 4253-4261.
25. M.C. Brelle, C.L. Torres Martinez, J.C. McNulty, Synthesis and characterization of CuxS nanoparticles. Nature of the infrared band and charge-carrier dynamics, Pure Appl Chem, 72 (2000) 101-117.
26. F. Zhang, S.S. Wong, Controlled synthesis of semiconducting metal sulfide nanowires. Chem Mater, 21 (2009) 4541-4554.
27. S. Jiao, L. Xu, K. Jiang, Well-defined non-spherical copper sulfide mesocages with singlecrystalline shells by shape-controlled Cu2O crystal templating, Adv Mater, 18 (2006) 1174-1177.
28. M. Anpo, S. Dohshi, M. Kitano, The preparation and characterization of highly efficient titanium oxide_ based photofunctional materials, Ann Rev Mater Res, (2005).
29. G. Hitoki, T. Takata, J.N. Kondo, (Oxy) nitrides as new photocatalysts for water splitting under visible light irradiation. Electrochemistry, 70 (2002) 463-465
30. A. Kar, Y.R. Smith, V. Subramanian, Improved photocatalytic degradation of textile Dye using titanium dioxide nanotubes formed over titanium wires, Environ Sci technol, 43 (2004) 3260-3265.
31. A.C. Herath, R.M.G. Rajapakse, A. Wicramasinghe, Photodegradation of Triphenylamino methane (magenta) by photosensitizer in oxygenated solutions, Environ Sci Technol, 43 (2009) 176-180.
32. Dasari Ayodhya, M. Venkatesham, A. Santoshi kumari, G. Bhagavanth Reddy, D. Ramakrishna, G. Veerabhadram, Journal of Experimental Nanoscience, http://dx.doi.org/10.1080/17458080.2015.1070312, 11(6) (2016) 418-432.
33. Dongqiang Han, Zhaofeng Wu, Zhihe Wang, Shaoguang Yang, Nanotechnology, doi:10.1088/0957-4484/27/13/135603, (2016).
34. A.E. Morales, E.S. Mora, U. Pal, "Use of diffuse reflectance spectroscopy for optical characterization of unsupported nanostructures," Revista Mexicana De Fisica S, (2007).
35. Senthilkumar, Vickraman, Ravikumar,"Synthesis of fluorine doped tin oxide nanoparticles by sol-gel technique and their characterization," Journal of Sol-

Gel Science and Technology, 53 (2010) 316-321.
36. F. Yakuphanoglu,"Electrical characterization and device characterization of ZnO microring shaped films by sol-gel method," Journal of Alloys and Compounds, 507 (2010) 184-189.
37. Yakuphanoglu, Mehrotra, Guta, M. Oz, "Nanofiber organic semiconductors: the effects of nanosize on the electrical charge transport and optical properties of bulk polyanilines," Journal of Applied Polymer Science, 114 (2009) 794-799.
38. J. Tauc, R. Grigorovici, A. Vancu,"Optical properties and electronic structure of amorphous germanium," Physica Status Solidi B, 15 (1996) 627-637.